Energy & Buildings 293 (2023) 113181

Contents lists available at ScienceDirect

# Energy & Buildings

journal homepage: www.elsevier.com/locate/enb

# Multi-objective study on an innovative system for domestic hot water production: A pilot building in Southern Europe

Aminhossein Jahanbin [a,b,*], Paolo Valdiserri [a], Giovanni Semprini [a]

[a] Department of Industrial Engineering (DIN), Alma Mater Studiorum - University of Bologna, Viale Risorgimento 2, 40136 Bologna, Italy
[b] CIRI - Centro Interdipartimentale di Ricerca Industriale Edilizia e Costruzioni, Alma Mater Studiorum - University of Bologna, Via del Lazzaretto 15/5, 40131 Bologna, Italy

ARTICLE INFO

*Keywords:*
Domestic hot water (DHW)
Storage tank
Energy storage
User behaviour
Dynamic simulation

ABSTRACT

The present study deals with a multi-objective analysis of an innovative decentralised system to produce and store domestic hot water (DHW), emphasising on the combined effects of the technological aspect, control strategy and user's behaviour. The proposed system, by relying on thermal energy storage, decouples energy production and demand while shaves peaks in the energy demand and, at the same time, provides more autonomy to users through local storages. To identify subtle interactions in components of DHW system, dynamic simulations are carried out by establishing a coupled TRNSYS-MATLAB code, calibrated and validated by experimental measurements. The energy analysis implies that the proposed system cuts the required annual electrical energy in half, of which up to 82% of needed primary energy is supplied from renewable sources, compared to previous electrical-decentralised system. The optimisation of the results through applying control strategies indicates that adopting a three-time charging scheme is advantageous in terms of providing a more stable temperature profile as well as a higher hot water temperature. Compared to an available-by-demand operation, this scheme reduces the required total annual electricity by 5.2 % and enhances total thermal loss from components up to 4.0%. Furthermore, a sensitivity analysis on the results emphasises the striking role of the user behaviour in electrical energy consumption either via draw-off temperature or adjusting the pre-defined temperature for activation of the built-in auxiliary heater.

## 1. Introduction

The European Union's policy objective is to move towards a low-carbon and sustainable development, with at least a 40% reduction in greenhouse gas emissions by 2030. The building sector is considered as one of the largest energy consuming sectors in European Union (EU) countries, using approximately 40% of the total energy demand [1]. The European Commission has set several long and short-term goals to increase energy efficiency in buildings as well as to reduce the energy consumed by the building sector. The building's energy consumption is assessed by regarding the required energy for heating, cooling, ventilation, lighting, and domestic hot water (DHW). The energy use for DHW production currently accounts for approximately 15–40% of the total energy need in dwellings, and this proportion is likely to be augmented; as the thermal resistance and air tightness of envelopes improve, the share of energy devoted to the space heating and cooling tends to go down, making DHW as a dominant energy load (as high as 50%) in high-performance buildings [2,3].

Nonetheless, recent research in reduction of energy use in building are focused primarily on reduction of space heating/cooling as well as ventilation needs, whereas current knowledge on the energy use and its optimisation for DHW production seems to be insufficient [4]. The efficiency of the DHW production and distribution varies to significant extent from case to case due to the large scattering of key parameters in the system such as piping layout and dimension, insulation level of pipework, size of storage tank, and time-dependency of DHW consumption profile [5]. Available studies in the literature indicate that the energy efficiency of DHW systems is surprisingly low and that a significant amount of heat is lost from the hot water before it reaches the draw-off points [6]. Hence, the DHW system may become the next bottleneck towards the low-energy buildings and sustainable development appointed by the European Commission. In this context, novel

* Corresponding author at: Department of Industrial Engineering (DIN), Alma Mater Studiorum - University of Bologna, Viale Risorgimento 2, 40136 Bologna, Italy.
*E-mail address:* aminhossein.jahanbin@unibo.it (A. Jahanbin).

https://doi.org/10.1016/j.enbuild.2023.113181
Received 3 January 2023; Received in revised form 9 May 2023; Accepted 16 May 2023
Available online 19 May 2023
0378-7788/

technologies and optimisation of the entire chain of the hot water production system are required to meet the ambitious goals of the future building regulations.

Indeed, optimisation strategies to reduce the energy footprint of DHW systems can be accomplished in different ways including the reduction in heat loss from hot water distribution system [7–9], efficient and sustainable DHW production technologies including renewable energy systems [10–12], recovering heat from wastewater at various level [13–15], and decreasing hot water consumption via behavioural and technological measures [16,17]. The earlier studies [18,19] indicated that the latter, namely occupants' behavioural measures, would have a significant impact on residential energy usage, compared to the type of heat source or supply temperature. However, it is not yet clear which strategy or what combinations has more potential and may lead to the best results for the least effort [20].

In the realm of optimisation and decarbonisation through DHW production technologies, particularly by employing the heat pump system and solar panel technology, there are several studies in the literature that focus on the integration of multiple technologies for the HVAC and DHW systems [11,21,22]. However, there are few studies on the specific-DHW technology topic aimed at reducing the energy footprint of hot water production system. For instance, Nimela et al. [23] analysed a new heating concept specially developed for DHW production in ground source heat pump (GSHP) system. The method was based on step-based heating of DHW, where the DHW is gradually heated from the inlet temperature of domestic cold water to the target temperature of DHW using a specifically designed GSHP system concept. The results demonstrated that the developed GSHP concept delivered up to 45–50% improvement in energy efficiency of the DHW heating process over the conventional GSHP application.

In another study, Corberan et al. [24] proposed a prototype dual source heat pump (DSHP) for DHW production. To assess the energy performance of the heat pump during 1 year of operation, an integrated system model has been developed in TRNSYS. They found that the DSHP system would be a profitable option compared to the ground-source heat pump (GSHP) system since the initial investment could be significantly reduced (up to a 30%) with a similar energy efficiency. Similarly, Liu et al. [25] proposed an inverter-driven heat pump with a multi-tubular tube-in-tube heat exchanger for domestic hot water supply. The obtained results showed that their developed heat pump for DHW can provide hot water at 65 °C with larger heating COPs (coefficient of performance) compared to the COPs obtained by three existing heat pump systems, including a *trans*-critical $CO_2$, R410A with an indirect contact coil and a HFC125 heat pump.

A numerical analysis of four different systems to produce DHW in a low energy multi-family residential building located in Poland was performed in [26]. Three investigated scenarios to produce DHW were tested: (i) district heating (DH) with heat exchanger, (ii) heat pump powered from wind turbines, PV cells, and grid, and (iii) natural gas high efficiency boiler. They concluded that the heat pump with renewable sources outperforms the boiler after 13 years. Based on their study, the heat pump and renewable electricity production can be economically competitive in areas without DH in the mid/long-term horizon of payback time of investment. Dongellini et al. [27] conducted a study on dynamic performance of the solar collector system in production of DHW to understand the effects of collector design, DHW profile and storage size on solar coverage fraction. They found that the annual and monthly solar coverage factor is strikingly influenced by the DHW profile consumption.

The literature review above implies that available specific-DHW studies have focused mainly on the production of hot water through a sustainable technology regardless of addressing the combined impacts of the proposed strategy on whole-DHW-system comportment, particularly in-building interactions. In fact, the role of integrated effects of technological aspects and in-building interactions, e.g., the control strategy or user behaviour, on the energy performance of DHW network are undeniable [20]. The present study aims to fill this gap by investigating performance of an innovative DHW system proposed for a pilot building with special emphasis on the role of control logic and user behaviour. This study is a part of the EU-funded H2020 innovation project entitled *e*-SAFE (Energy and seismic affordable renovation solutions) [28], appointing a central role to heat storage systems by developing technologies that enable effective integration and communication in the DHW production.

In this context, firstly, the proposed model and its characteristics to produce DHW in a pilot building, located in Southern Italy, are described in detail. Then, the energy analyses of the DHW system are performed through a dynamic simulation model, established in TRNSYS software and coupled to a MATLAB code simulating the DHW consumption profile. The numerical model is validated and calibrated against experimental measurements. The energy optimisation of proposed system is carried out through a series of control strategies. Finally, the role of user behaviour in the energy saving for proposed system is evaluated. The findings of the present study are expected to provide insights into the future design of efficient and sustainable DHW systems.

## 2. Materials and methods

### 2.1. Pilot building description

The *e*-SAFE project deals with solutions for the energy and seismic deep renovation of reinforced concrete (RC) framed buildings in the European countries, addressing both the energy performance of the building envelope and the heating and cooling of the indoor spaces to boost the decarbonisation of inefficient European building stock. However, the present study focuses only on the proposed DHW solution for the pilot building.

The pilot building is a residential building having five floors and ten dwellings (32 occupants), located in Catania, Italy. Fig. 1 displays the pilot building under study. The retrofit solution for DHW system proposes to remove actual electric boilers and to install a centralised PV-fed air source heat pump system relying on thermal energy storage to decouple energy production and demand while also shaving peaks in the energy demand. In addition, it offers innovative slim decentralised plug-and-play tanks to produce and store DHW, hereafter called *e*-TANK, providing a higher thermal efficiency and, at the same time, a greater users autonomy through local storages installed in each dwelling.

Fig. 2 illustrates the layout of proposed model for DHW system. Each apartment is equipped with a wall-mounted *e*-TANK system with an internal helical heat exchanger which is connected to a 2-pipe hot water network. The *e*-TANK system is installed on the lateral wall of the external balcony due to existing positions of main pipe networks, reducing installation works, minimising the installation costs and disturbance for the occupants.

The circuit fluid (technical water) is produced by a mono-block air-to-water heat pump, coupled to an inertial storage tank, and via circulating pumps and supply network feeds the heat exchanger of *e*-TANK. After transferring heat to the aqueduct (cold water), the circuit fluid is discharged from *e*-TANK to the main storage tank through the return piping network. The distribution network can be used for the charging of DHW storage tanks and can be also utilised for the heating purpose. In both cases, the 2-pipe network can work at high temperature during charging periods for few hours a day, resulting in lower heat losses from the distribution network.

The pilot building is equipped with polycrystalline photovoltaic (PV) modules on rooftop (36 panels), characterised by a net absorbing surface of 1.46 $m^2$ and a peak power of 220 W, to fulfil the legal obligations to cover the renewable energy system (RES) quota, namely 60%. Electricity produced by solar modules can be either consumed instantaneously by the heat pump system or stored in a considered 20 kWh BESS (battery energy storage system).


**Fig. 1.** The pilot building under study.

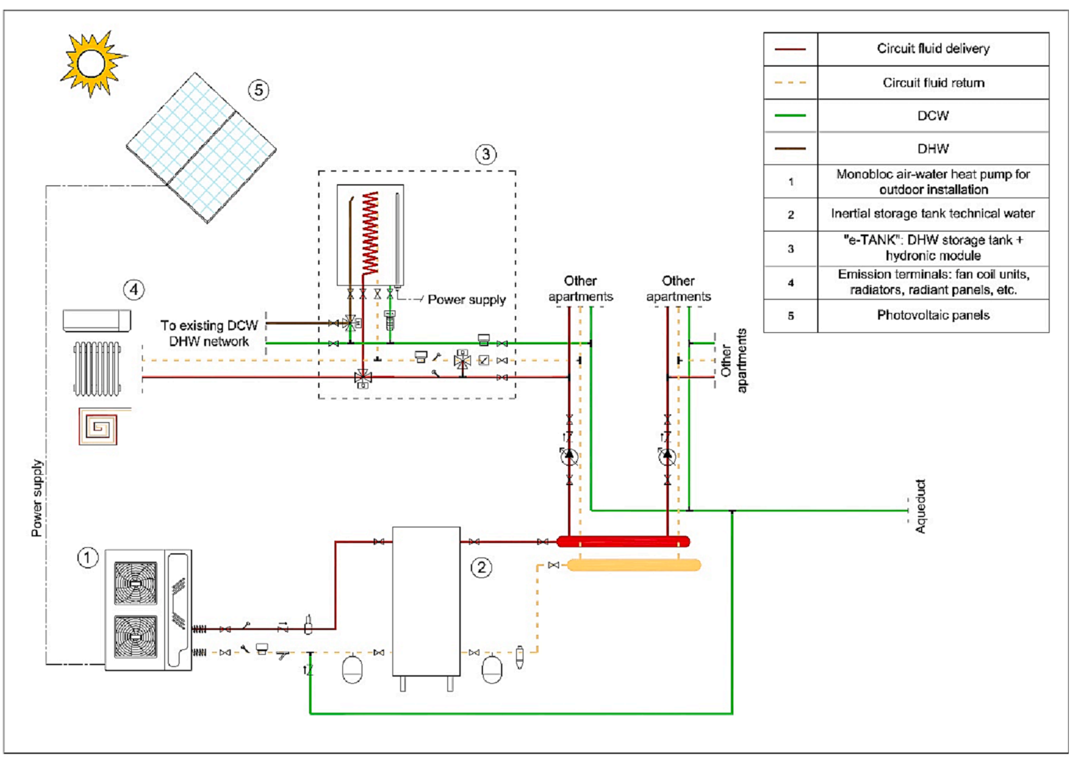


**Fig. 2.** Technical scheme of the proposed model for DHW system.

### 2.2. e-TANK system

The *e*-TANK system consists of two main subsystems, namely the “storage tank” and the “hydronic module”, designed and manufactured by PINK GmbH. Both components are connected and mounted on a steel frame, which then are fixed on existing walls. The storage tank, with a volume of 140 *l* and height of 1.72 m, made of stainless steel-1.4571 (V4A), has a flat design built with pieces of vertically orientated pipes welded together with horizontal connecting pipes on the top and the bottom, as illustrated in Fig. 3 (a and b). The central pipe was equipped with a screwed flange and equipped with a helical coil heat exchanger which is connected to a 2-pipe hot water network system powered by the central heat pump. The integrated coil heat exchanger, made of molybdenum-bearing austenitic stainless steel, was located at the central storage pipe, having the heat transfer area of about 2.0 m$^2$ and a total length of coiled tube equal to 17.88 m. Moreover, the storage tank was equipped with an internal sensor reaching the entire storage height with an inner diameter of 12 mm. Regarding tank insulation, in addition to the conventional insulation by means of a PU foam, a further 8 cm layer of vacuum insulation panels (VIP) were applied to the two largest


**Fig. 3.** Characteristics of the *e*-TANK system: Schematic and dimensions (a), storage prototype (b), hydronic unit (c), control cabinet (d), auxiliary electrical heater (relay) (e), ultrasonic heat meter (f), cold-water flow sensor (g), and three-way diverter valve + actuator (h).

surfaces of the tank, resulted in a stand-by thermal loss equal to 0.92 kWh/day.

Details of the hydronic unit and its main components are illustrated in Fig. 3(c-g). In the hydronic unit, a control cabinet (Fig. 3(d)) was installed, where the electric and electronic cables of the installed components were wired. The control cabinet also includes the PLC (programmable logic controller) system, in which the control and monitoring activities can be realised. Fig. 3(e) shows the built-in auxiliary heater (relay) which was screwed into the tank via 1 ½“coupling. The auxiliary heater has 1.5 kW power and consists of three U-shaped elements fitted in a brass nipple. It was equipped with an electromechanical temperature controller and a safety temperature limiter according to EN 14597 [29]. The main logic of integrating the auxiliary heater to *e*-TANK is to facilitate fulfilling certain regulations regarding *Legionella pneumophila*, such as EN 806–1 [30], by boosting the tank temperature via an optional electrical heating element. Furthermore, it allows users heating up the water outside the central plant charging schedule and maintaining the tank temperature periodically higher. The ultrasonic heat meter, illustrated in Fig. 3(f), measures the heat load and its data logger provides values in a 1-min interval. The adopted cold-water meter (Fig. 3(g)) is an electronic ultrasonic meter, and the installed 3-way diverter valve regulates the mass flow and the corresponding thermal load into the supply lines of the DHW-circuit via an electrical ON/OFF actuator (Fig. 3(h)).

### 2.3. Dynamic simulation model

The energy performance of DHW network was investigated by means of a dynamic simulation model implemented in TRNSYS software which was coupled to a MATLAB code simulating the DHW consumption profile in each apartment. The dynamic simulations were carried out for duration of one year using a 1-min interval (time step), as suggested in [31] for the dynamic simulation of DHW systems.

According to the layout of the proposed model (Fig. 2), the total length of supply and return piping network is equal to 198.6 m. The piping network consists of tubes with different internal diameters, varying between 16.2 mm and 51.4 mm, and an insulation thickness ranging from 19 mm to 33 mm, according to Italian regulation DPR 412/93 [32]. In the TRNSYS model, a Type 31 model was employed for the piping network and types 649 and 647 were utilised for mixing and diverting valves, respectively. The weather data Type-15 was adopted for the external temperature as well as for the aqueduct temperature, connected to relevant components. The mean annual outdoor temperature and aqueduct (mains) temperature in the pilot building was equal to 17.87 and 19.22 °C, respectively.

The model Type 534-Coiled was employed to simulate features of the *e*-TANK, calibrated in charging and discharging process by experimental measurements, which will be presented in section 3. The *e*-TANK with volume of 140 *l* consists of two inlet and two outlet flow ports: an inlet for aqueduct and an outlet for DHW (to user), and inlet and outlet ports for supplied and discharged circuit fluid through the heat exchanger. According to the measured data, the thermal loss coefficient of *e*-TANK is equal to 0.56 W/m$^2$K. Moreover, by using a thermostatic valve (Type 953), it was assumed that the draw-off temperature in preliminary simulations is equal to 38 °C. However, the role of variation in draw-off temperature on energy result is addressed later. The heat generated by auxiliary heater inside e-TANK was modelled by inserting a heat source input to specified nodes, according to the geometry and power of the electrical heater.

The circuit fluid is supplied to each *e*-TANK with a flow rate of 300 kg/h through two circulating pump units (Type 743), i.e., each pump for five apartments located on each side of the building, with the rated power and mass flow rate of 50 W and 1500 kg/h, respectively. The main storage tank was modelled by Type 4c component, with the volume of 1000 *l*, height of 2.4 m and loss coefficient of 0.40 W/m$^2$K, with a varying set-point temperature based on the heat pump performance. The heat pump is air-to-water system with nominal heating capacity of 26.0 kW, COP of 3.10 and SCOP of 4.51. The maximum water temperature supplied by the heat pump is equal to 65 °C for the outdoor temperature between 5 °C and 19 °C. For the outdoor temperature between −15 °C and 5 °C, and between 19 °C and 43 °C, the supply temperature varies in the range of 55 °C and 60 °C, according to the technical data of manufacturer.

Considering the outlet water temperature curve for the heat pump, the set-point temperature of *e*-TANK in cold seasons was regarded equal to 50 °C, whereas that in warm seasons was 45 °C. An ON/OFF controller (Type 2) was employed for both central storage and *e*-TANKS to regulate the set-point temperatures in upper and lower limit of ± 2.5 °C. In addition, the control logic of DHW system, including activation times and signal controls, was modelled by utilising equation/calculator unit, season scheduler Type 515 and timer Type 21.

The domestic hot water demands were regulated based on the number of occupants in each apartment, the seasonal (monthly) consumption factor, and the daily (hourly) consumption profile. In order to model the DHW consumption profile, a MATLAB code was developed and linked to the TRNSYS model by introducing a NORMRND function. This function generates random samples from a normal (Gaussian) distribution by a mean and a standard deviation parameter, allowing more realistic simulation of the daily DHW consumption for different daily time slots. The MATLAB code reads the number of occupants in each apartment from the TRNSYS, and then at each time step, by taking into account the monthly factor and hourly profile, returns a value as a consumption to the TRNSYS.

According to the literature data [33], the mean daily DHW consumption for each occupant was considered equal to 45 *l*, varying slightly in each month, i.e. divided on the basis of cold and warm seasons [34]. Furthermore, in the daily consumption profile, it was assumed that peaks of the daily consumption profile occur in the morning between 06:00 and 10:00 (45% of total daily consumption) as well as in evening between 18:00 and 22:00 (25% of total daily consumption) [35]. To have a plausible comparison between energy results, an identical annual simulated DHW consumption profile was inserted in TRNSYS model as an input file for comparative case studies.

The hourly electricity production from PV panels was calculated by using the EU tool called “PVGIS” [36], rendering the hourly global irradiation values (Wh/m$^2$) from the “SARAH 2″ database. In the calculations, the total number of panels was considered equal to 36 with the peak power factor of 0.16 kW/m$^2$, system efficiency factor of 0.80, absorbing surface area of 1.46 m$^2$, and reference solar irradiance of 1.0 kW/m$^2$. Furthermore, the conversion factors for estimating the required primary energy as well as the $CO_2$ emission were adopted from the Italian Regional Legislative [37].

### 2.4. Control logic

Regarding the control strategy, the circuit fluid is supplied to *e*-TANKs via the circulating pump in pre-defined activation time slots. For baseline simulations, two typical charging periods were firstly considered, namely continuous operation (24 h), i.e., available-by-demand scheme, and daytime charging (06:00–22:00). Then, the charging scheme is optimised based on the DHW consumption profiles and energy demand. Furthermore, via an activation signal control, the circulating pump is activated only when the temperature of main storage be higher than set-point temperature of *e*-TANKs, regardless of the charging scheme.

When the temperature of central storage decreases to a value lower than its set-point temperature due to charging of *e*-TANKs, the heat pump is activated and feeds the central storage. The set-point of main storage tank varies with the outlet water temperature of heat pump. For baseline simulations, the set-point temperature of main storage was considered as 4.0 °C lower than the outlet water temperature of heat pump. In addition, it was considered that the heat pump system works in accordance with the activation times of the circulating pump. However, for two or three charging periods per day, it was considered that the heat pump would work continuously from the start of the first available charge to the end of the last one, in order to minimise ON/OFF cycles of the heat pump.

During the activation timespan of the circulating pump in each charging scheme, if the temperature of any *e*-TANK drops below the set-point temperature, due to either draw-off or thermal loss, the electronic valve inside the hydronic module immediately opens and charges the demanded *e*-TANK to reach the set-point temperature. If the temperature of *e*-TANK outside of the charging time slot drops below a pre-defined value by user (occurs mostly after midnight), the auxiliary heater is activated. The pre-defined temperature for activating the auxiliary electrical heater in baseline simulations was considered to be 39 °C (±1 °C). For the energy optimisation of the results, the effects of different activation temperatures on performance of DHW system is examined. It also should be mentioned that the required energy for *anti-legionella* treatment by electrical heater was not considered in dynamic simulation due to the diversity of regulations.

## 3. Validation of dynamic simulation code

As the main component of the proposed DHW system, the developed *e*-TANK model in dynamic simulations was calibrated and validated with results obtained through the experimental campaign. In this context, the numerical model was calibrated in terms of the tank insulation, stand-by thermal loss, temperature stratification, and charging/discharging capacity. In the following, the validation of the model in both charging and discharging processes are demonstrated.

### 3.1. Charging process

The charging process was measured for different charging conditions regarding the inlet temperature and flow rate of heat exchanger. For model calibration, the upper and lower limit of charging flow rate, i.e., 150 and 300 kg/h, at two supply temperatures, namely 45 and 65 °C were considered. However, for the sake of brevity, one combination of temperature and flow rate is presented here. The nodal temperature inside the *e*-TANK was measured by means of a sensor tube with internal diameter of 12 mm and a height equal to that of the tank with accuracy of ± 0.1 °C, as illustrated in Fig. 3(a). Five nodal temperatures were regarded to be measured, in which the temperature of the highest node is identical to DHW temperature delivered to users.

Fig. 4 illustrates the time evolution of *e*-TANK's nodal temperature for the case with mass flow rate 300 kg/h and supply temperature of 45 °C. The figure demonstrates the transient temperature stratification inside the tank and shows that the full-charging process of *e*-TANK under mentioned charging condition takes around 70 min. However, the temperature of DHW at outlet port reaches its maximum value much sooner, namely at $\tau = 40$ min. The figure shows a good agreement between experimental and numerical results. The normalised-root-mean-square-deviation (NRMSD) of the simulated DHW profile from experimental results is 0.91% with maximum discrepancy of 2.63%.

Similarly, Fig. 5 compares the measured and simulated return temperature and charging load of the *e*-TANK during half an hour, for supply temperature of 45 °C and volume flow rate of 300 kg/h. The figure shows that, for a given supply temperature, a lower return temperature is associated to a larger charging load. It can be observed that the maximum charging load is slightly less than 9.5 kW, occurring in the very first minutes of the charging process. A comparison between numerical and experimental results reports a NRMSD equal to 2.16 and 3.79 % for the return temperature and charging load, respectively.

### 3.2. Discharge capacity

The discharge capacity of the tank was evaluated by considering a 3-way thermostatic mixing valve connected to the *e*-TANK at outlet port in order to keep the tap water temperature at 40 °C, whereby hot water is mixed down with the cold water at 14 °C. Fig. 6 compares the discharge capacity of the *e*-TANK for various supply temperatures, yielded by both experiments and simulations. The figure shows that the discharge capacity is a linear and increasing function of the tank temperature at DHW outlet; for a 1 °C increase in supply temperature, the discharge capacity enhances 0.24 kWh. A comparison between experimental and numerical results shows a negligible discrepancy for each case, ranging between 0.5 and 1.4 %.

## 4. Results

### 4.1. Energy performance analysis

The DHW consumption profile by each apartment is demonstrated in Fig. 7, for different daily time slots in a typical winter (a) and summer (b) day. A comparison between DHW profiles shows that each apartment has a different consumption pattern; indeed, the developed MATLAB code takes into account the number of residents, monthly variation factor, and specified time slots in which the DHW is demanded. For instance, apartment No.1 has the highest total consumption, either in summer or in winter, since it has the maximum number of occupants, namely 5 occupants. The developed code for the DHW consumption profile renders a random value for each time slot in a predefined deviation threshold even for an identical number of residents and season. An evident for this is the consumption profile in apartments 3 and 8, where both cases have 4 residents. However, it should be noted that the mean annual consumption for both apartments (and for others) is 45 *l*/person/day. Furthermore, the figure shows that the trend of consumption profile

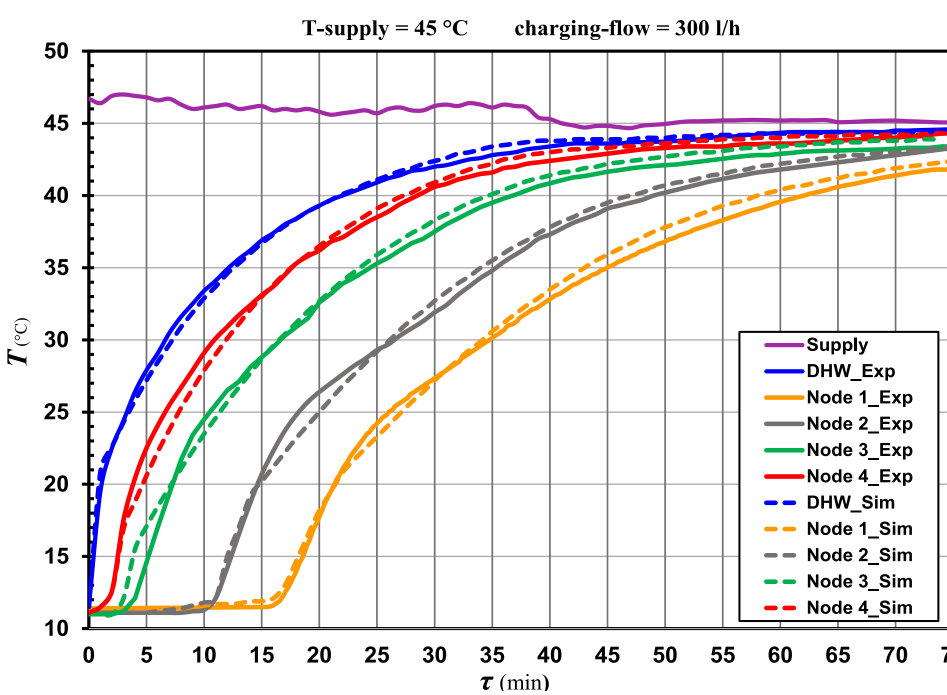


**Fig. 4.** Time evolution of *e*-TANK's nodal temperatures: Experiments vs. simulation.

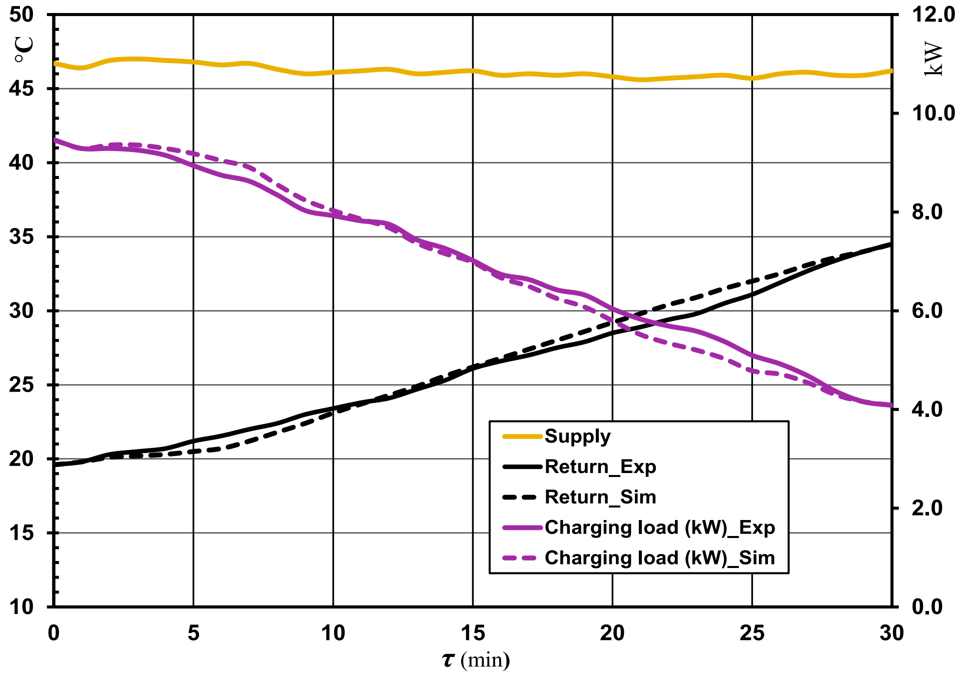


**Fig. 5.** A comparison between measured and simulated time evolution of the return temperature and charging load of the *e*-TANK.

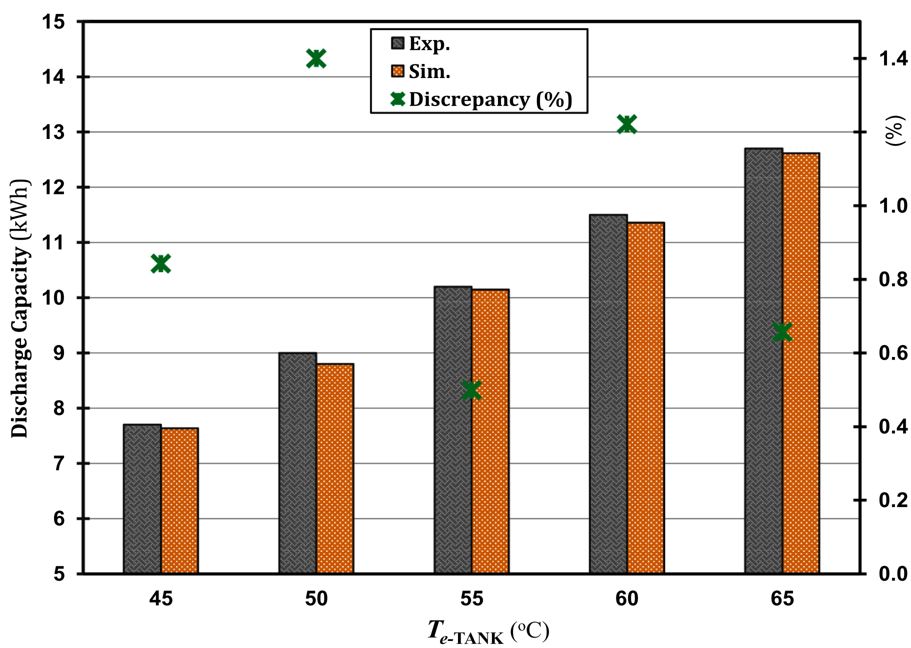


**Fig. 6.** Discharge capacity of *e*-TANK for different charging temperatures: Experiments vs. simulations.

in the summer is similar to that in the winter with slightly lower values.

Fig. 8 compares the total daily consumption of DHW, i.e., for 10 apartments with 32 occupants, in a typical winter and summer day. For both seasons, it shows that there are two peak timespans for DHW demand; first and the greater one is in the morning period, namely between 06:00 and 10:00, and another one in the evening between 18:00 and 22:00. The total daily consumption profile implies that the highest hourly consumption in winter reaches 238 L while in summer it is slightly lower than 190 L, both in the early morning. According to the figure, the mean daily consumptions per person in the winter and summer day (extreme values) are 49.58 and 39.54 L, respectively.

To highlight effects of the DHW demand profile in each apartment on the supplied hot water temperature, Fig. 9 compares the daily temperature variation at outlets of *e*-TANKs and the main storage in a typical winter (a) and summer (b) day. Three apartments with minimum (1), intermediate (3) and maximum (5) number of occupants were selected. A comparison between temperature profiles in winter and summer days shows a higher supply temperature by main storage in winter, due to performance of the heat pump, and, consequently, a higher set-point temperature of *e*-TANK. For a given set-point temperature of *e*-TANK, the figure evidently shows impact of the level of consumption on the variation of temperature profile; for both seasons, the figure indicates that the lower the number of occupants (lower consumption), the higher the mean tank temperature as well as the lower the temperature

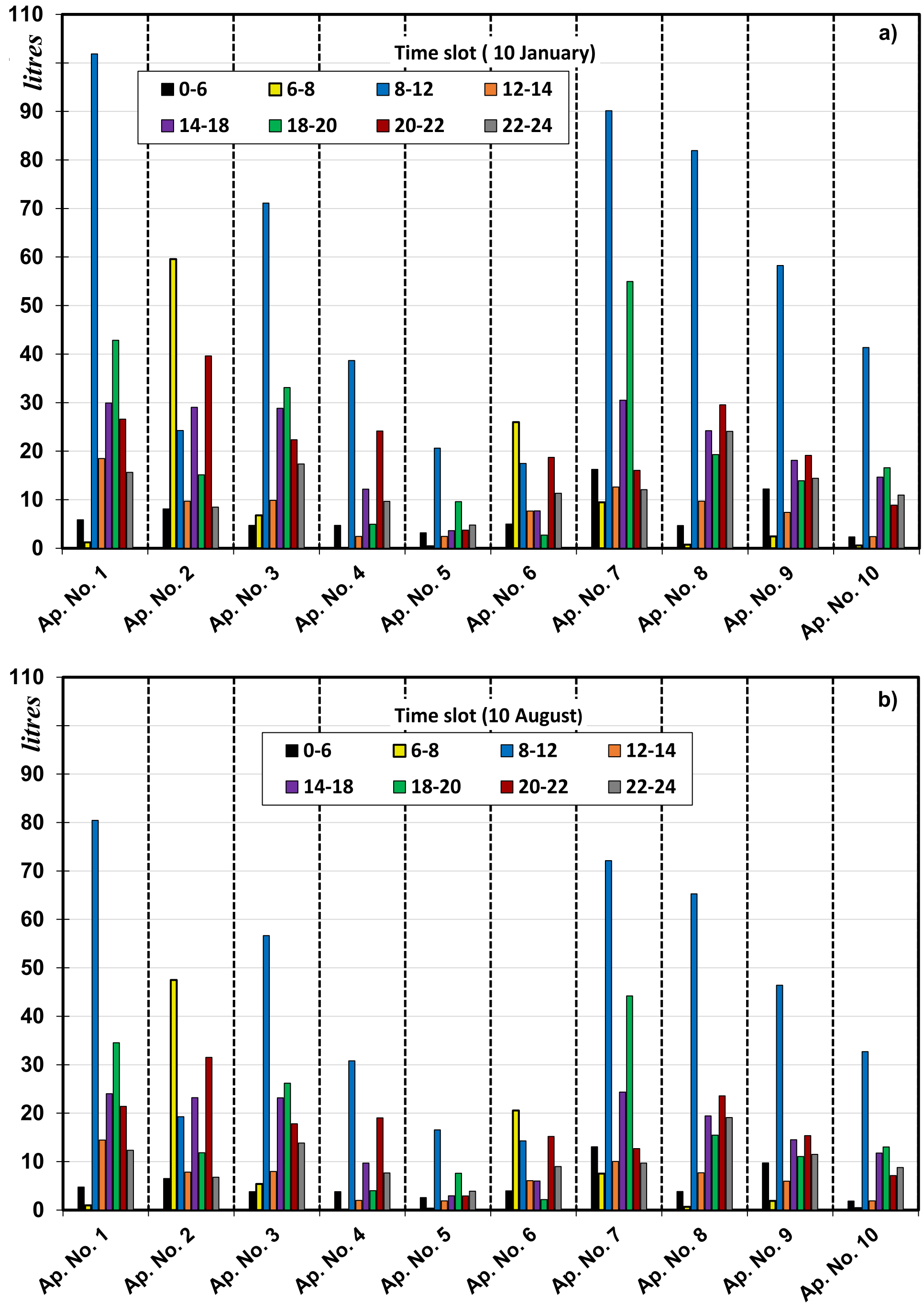


| Apartment No. | 1 | 2 | 3 | 4 | 5 | 6 | 7 | 8 | 9 | 10 |
|---|---|---|---|---|---|---|---|---|---|---|
| Number of occupants | 5 | 4 | 4 | 2 | 1 | 2 | 5 | 4 | 3 | 2 |

**Fig. 7.** DHW consumption profile by apartment in different daily time slots of a typical winter (a) and summer (b) day.

oscillations. For instance, the daily temperature profile in the winter for an apartment with 3 residents reaches five peaks (due to the DHW demand and heat exchanger charging) with the mean temperature of 49.9 °C, while that in the apartment with 1 occupant reaches one peak with the mean temperature of 50.6 °C. However, temperature profiles show that *e*-TANK system decouples the energy demand for each dwelling and maintains the temperature in the pre-defined range, unlike the common centralised systems having a non-negligible difference in hot water temperature delivered to each dwelling.

Fig. 10 compares the annual energy performance of the proposed system with the current decentralised DHW system in pilot building consisting of a cylindrical tank in each apartment with an electrical resistance having 2 kW power. In order to have a logical comparison between energy performance in previous and proposed ones, the set-point temperature, insulation characteristics and volume of tank in decentralised system were considered identical to those of the proposed system. Moreover, for the charging period of *e*-TANK through the circulating pump, two schemes were considered: available-by-demand

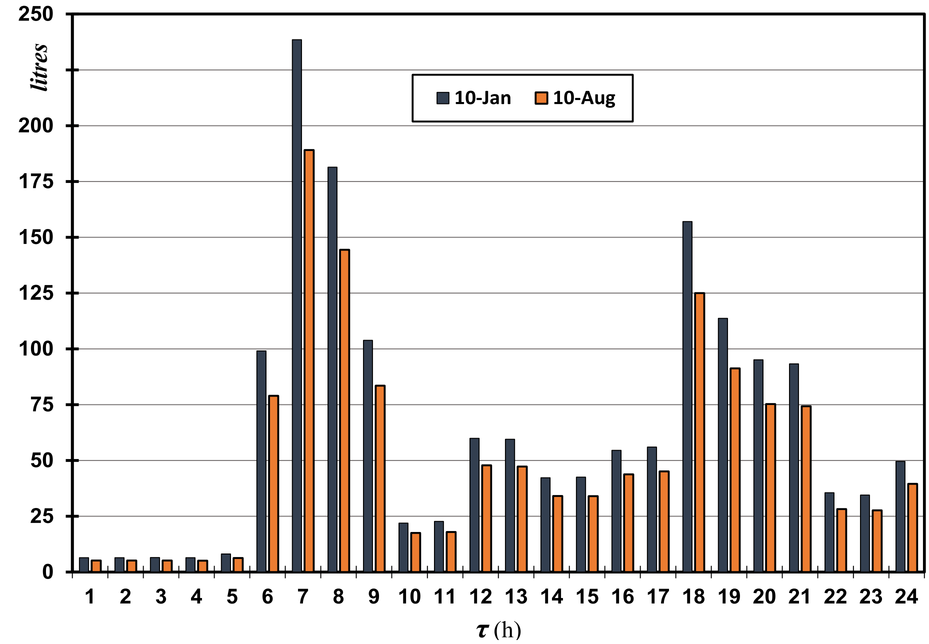


**Fig. 8.** Total daily consumption of DHW in the pilot building (10 apartments with 32 occupants) in a typical winter and summer day.

(24 h) and daytime charging (06:00–22:00).

The results of Fig. 10 imply that the total annual electrical energy consumption of DHW system in decentralised system is more than twice than that in the proposed system, regardless of the charging scheme, corresponding to more than 2885 kg higher annual $CO_2$ emission. However, decentralised system shows 76.1 and 73.2 % lower total thermal loss, compared to these cases, which is due to not having thermal loss from the distribution system and the main storage. A comparison between results for the proposed system under two charging scenarios indicates that daytime charging can be beneficial in terms of either energy saving or thermal loss from the DHW components. The energy optimisation of the system according to the circulating pump charging scheme is discussed in detail in Section 4.2.

Although the proposed DHW system shows advantages in terms of energy consumption with respect to the previous system, it is of great importance to address the share of renewable energy source in the DHW system for pilot building. The charts in Fig. 11 demonstrate the annual required primary energy (*PE*) and the share of renewable source in the proposed DHW system for three scenarios: The total electrical energy required for DHW system is supplied by the external grid, by utilising PV system (without battery), and by using PV system in conjunction with the battery storage. The figure shows that the total primary energy for the external grid case is about 27.7 MWh of which 54.8% is renewable. The use of PV reduces the amount of primary energy to 24.6 MWh with renewable share of 66.4%. For the proposed case, namely utilising the battery to store the PV electricity, the total primary energy is further reduced (20.1 MWh) with renewable quota of 82.4%.

### 4.2. Optimisation of energy consumption

Indeed, energy optimisation of a DHW system is obtainable through a series of measures enhancing the thermal performance of DHW systems' components. Nevertheless, the present study seeks to demonstrate the striking role of the control strategies in energy optimisation of the proposed DHW system. In the previous section, the energy performance data were presented for two default working conditions of the circulating pump unit, namely for available-by-demand case (24 h) and daytime charging scheme (06:00–22:00). Table 1 shows how various charging periods of the *e*-TANK can affect the annual electrical energy consumption of the heat pump ($E_{el\text{-}HP}$), auxiliary heater ($E_{el\text{-}ER}$), circulating pumps ($E_{el\text{-}cir}$), total electricity consumption ($E_{el\text{-}tot}$), total thermal energy produced ($E_{th\text{-}tot}$), and total thermal loss of the system ($E_{loss\text{-}tot}$). Moreover, it reports the decrement percentage of total electrical energy consumption ($\delta_{el\text{-}tot}$) with respect to the available-by-demand case (*S*-0), defined as:

$$\delta_{el-tot} = \frac{E_{el-tot,S-0} - E_{el-tot,S-i,j}}{E_{el-tot,S-0}} \times 100 \tag{1}$$

as well as the ratio of thermal loss to the produced thermal energy in percentage for each scenario denoted by $\varepsilon_{loss}$:

$$\varepsilon_{loss} = \frac{E_{loss-tot,S-i,j}}{E_{th-tot,S-i,j}} \times 100 \tag{2}$$

Apart from *S*-0 and *S*-1.1, twelve different charging scenarios have been selected in two categories (each six): two times charging per day (*S*-2) and three times charging per day (*S*-3), for an identical total hours of charging. In terms of energy optimisation, the time slots were selected in the way to be matched with peak consumption periods, according to Fig. 8.

The table shows influential role of the employing a pre-defined charging period (either two or three times per day) not only on the total electrical energy consumption, but also on the improvement of the heat loss from the DHW components, compared to the scenario of continuously activated pump, namely *S*-0; it reports up to a 5.3% (*S*-2.2) saving in electrical energy, equal to 342 kWh per annum, and up to a 5.1% decrement in total thermal loss from DHW system (*S*-2.1), for a given set-point temperature. It is noticeable to mention that, in preliminary analyses, the effect of different total hours of charging in *S*-2 and *S*-3 scenarios was investigated and it turned out that the presented total hours, namely 7 h, is the most efficient one in terms of energy efficiency of both the heat pump and the auxiliary heater.

A comparison between various cases indicates that while *S*-2 cases show a larger decrement in energy consumption of the heat pump, compared to *S*-3 cases, they should utilise much more the auxiliary heater for maintaining the required set-point temperature. Nonetheless, there is not a significant difference between these cases in terms of the energy consumption of circulating pump and total thermal loss. The results clearly indicate the sensitivity of the DHW energy consumption to the charging scheme of *e*-TANK and, therefore, the importance of

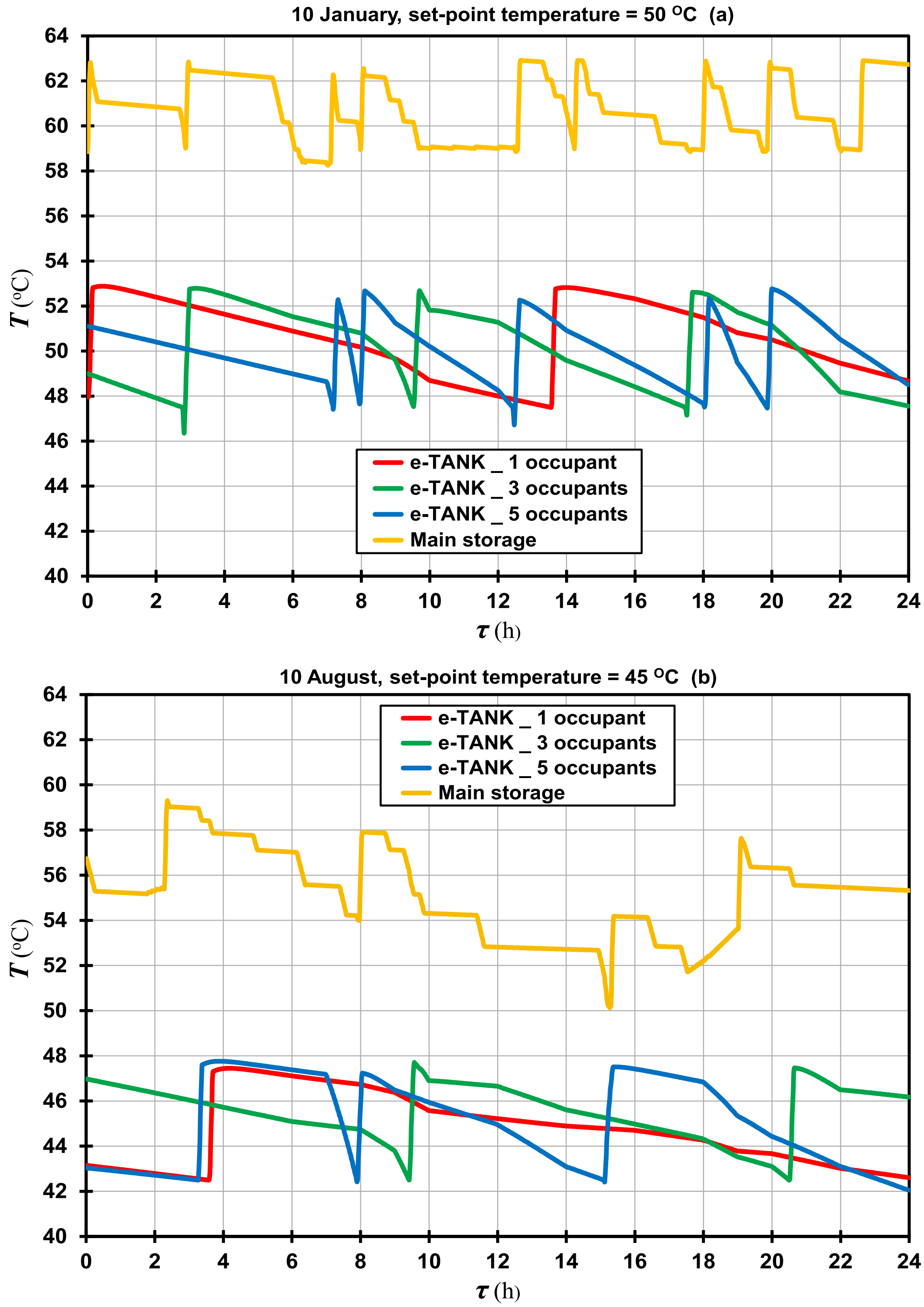


**Fig. 9.** Temperature variation at the outlet (supply) of *e*-TANKs and main storage in a typical winter (a) and summer (b) day.

adjusting the charging period to users' consumption profile in order to optimise the energy consumption.

In terms of the total energy consumption ($E_{el\text{-}tot}$), the table indicates that cases *S*-2.1 and *S*-2.2 in two times charging, and *S*-3.4 and *S*-3.5 in three times charging, can be considered as the most efficient ones, with a negligible quantitative difference. However, to choose the most optimal scenario, it would be beneficial to compare the DHW temperature profile in these cases. Fig. 12 illustrates the DHW temperature profile for these cases in a typical winter day, for an apartment with 5 occupants (most critical case). The figure clearly shows that employing three times charging (*S*-3) is more advantageous since it provides not only a more stable DHW temperature profile, but also the DHW with a higher temperature, i.e. up to 3.2 °C on daily-average basis. This issue can be explained by the fact that, in *S*-2 cases, there is the lack of *e*-TANK charging in midday, when there are DHW demands by users (see Figs. 7 and 8), which causes a further drop and oscillation in DHW temperature, resulting in a higher annual consumption of the auxiliary heater, compared to *S*-3 cases. In addition, employing three times charging could be more beneficial in terms of a direct harvesting of the PV energy in midday.

Elaboration of results shows that the presence of the built-in auxiliary heater also leads to a higher tank temperature, compared to the situation without utilising that in the proposed DHW system. To provide a better demonstration on the efficacy of utilising the auxiliary heater, Fig. 13 compares the temperature of DHW system with (*ER*) and without auxiliary heater (*wER*) in a typical summer and winter day, for a case with the minimum energy consumed by the auxiliary electrical heater, namely *S*-3.4 (Table 1). In both winter and summer days, the figure

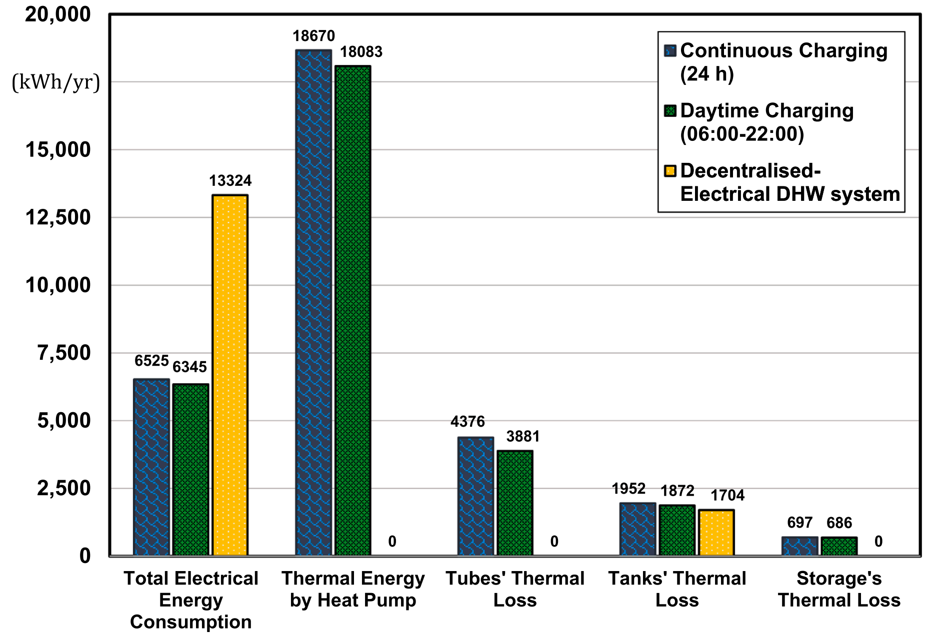


**Fig. 10.** Comparison of the annual energy performance between the proposed DHW system under available-by-demand (24 h) and daytime (06:00–22:00) charging schemes and the current decentralised-electrical DHW system.

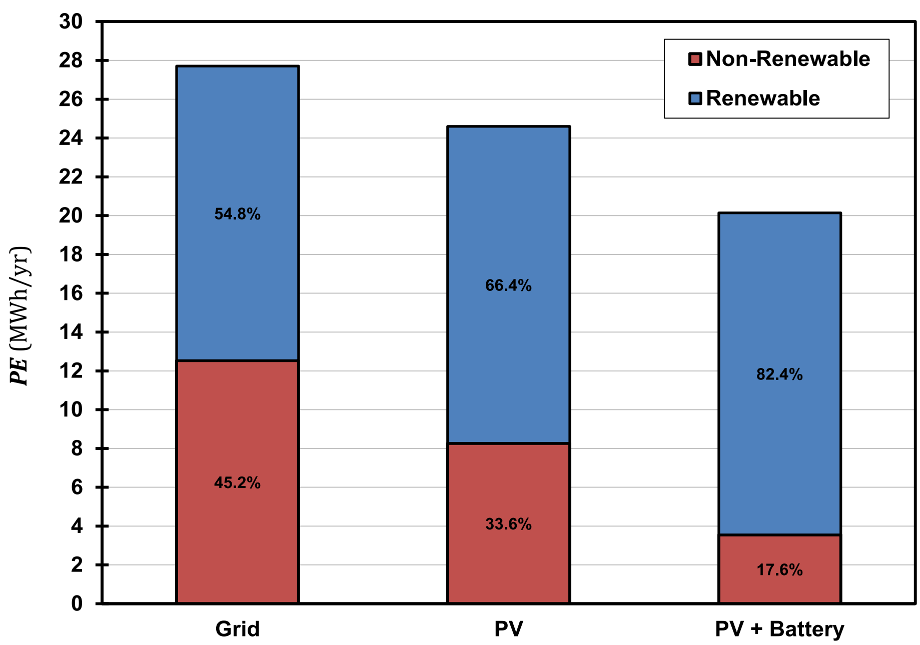


**Fig. 11.** The annual required primary energy and the share of renewable source in proposed system for DHW production under different electricity supply scenarios.

evidently shows that in time-spans out of the charging periods, particularly at night, the *ER* case renders DHW with a higher temperature than *wER*; the mean daily temperature differences between two cases in the winter and summer day are 0.4 and 0.3 °C, respectively. It should be noted that this temperature difference stands for the most optimal scenario and it could be higher for other scenarios. A comparison of the annual energy data implies that the auxiliary heater requires 46 kWh/yr in *ER* scenario. However, the annual consumption of the heat pump in the presence of auxiliary heater is 27 kWh/yr lower than that in *wER* case. Thus, providing the afore-mentioned facilities by using auxiliary heater is at the cost of only 19 kWh higher annual electricity consumption.

In this context, the pre-defined temperature by user for activation of the auxiliary heater is also a parameter that can play an important role in energy saving. Fig. 14 shows the impact of the set-point temperature of auxiliary heater ($T_{ER}$) on annual energy consumption of the built-in electrical heater ($E_{el\text{-}ER}$) and heat pump ($E_{el\text{-}HP}$) under two charging scenarios, namely *S*-2.1 and *S*-3.4. The figure indicates that an increment in the $T_{ER}$ increases the share of energy consumption by the electrical auxiliary heater, but, at the same time, it decreases the share of energy consumption by the heat pump. It also shows that, for a given set-point temperature ($T_{ER}$), *S*-2.1 requires by far larger $E_{el\text{-}ER}$ compared to *S*-3.4, confirming the validity of results in Table 1 for different values of $T_{ER}$. On the other hand, the energy consumption of heat pump ($E_{el\text{-}Hp}$) in *S*-2.1 is lower than *S*-3.4, as reported in Table 1. In terms of the energy optimisation, the figure demonstrates that the rate of changes in energy

**Table 1**
Comparison of the annual energy performance for different charging schemes.

| Scenario | Charge / day | Charging period | $E_{el\text{-}HP}$ (kWh) | $E_{el\text{-}ER}$ (kWh) | $E_{el\text{-}cir}$ (kWh) | $E_{el\text{-}tot}$ (kWh) | $\delta_{el\text{-}tot}$ (%) | $E_{th\text{-}tot}$ (kWh) | $E_{loss\text{-}tot}$ (kWh) | $\varepsilon_{loss}$ (%) |
|---|---|---|---|---|---|---|---|---|---|---|
| S-0 | – | 00–24 | 6,354 | 0 | 97 | 6,451 | 0.0 | 18,670 | 7,045 | 37.7 |
| S-1.1 | 1 | 06–22 | 6,153 | 22 | 72 | 6,247 | 3.2 | 18,083 | 6,439 | 35.6 |
| S-2.1 | 2 | 06–10, 18–21 | 5,938 | 157 | 40 | 6,135 | 4.9 | 17,042 | 5,551 | 32.6 |
| S-2.2 | 2 | 06–09, 17–21 | 5,885 | 182 | 42 | 6,109 | 5.3 | 17,089 | 5,626 | 32.9 |
| S-2.3 | 2 | 06–09, 18–22 | 5,871 | 328 | 44 | 6,243 | 3.2 | 16,974 | 5,644 | 33.3 |
| S-2.4 | 2 | 07–10, 17–21 | 5,839 | 259 | 43 | 6,141 | 4.8 | 17,032 | 5,619 | 33.0 |
| S-2.5 | 2 | 05–09, 18–21 | 5,948 | 227 | 39 | 6,214 | 3.7 | 17,003 | 5,595 | 32.9 |
| S-2.6 | 2 | 07–10, 18–22 | 5,895 | 234 | 43 | 6,172 | 4.3 | 17,095 | 5,675 | 33.2 |
| S-3.1 | 3 | 06–09, 12–14, 19–21 | 6,018 | 165 | 49 | 6,232 | 3.4 | 17,414 | 5,925 | 34.0 |
| S-3.2 | 3 | 06–09, 11–13, 18–20 | 6,005 | 82 | 45 | 6,132 | 4.9 | 17,281 | 5,713 | 33.1 |
| S-3.3 | 3 | 06–09, 12–14, 18–20 | 6,031 | 72 | 47 | 6,150 | 4.7 | 17,425 | 5,839 | 33.5 |
| S-3.4 | 3 | 06–10, 12–13, 18–21 | 6,024 | 47 | 46 | 6,117 | 5.2 | 17,506 | 5,903 | 33.7 |
| S-3.5 | 3 | 07–10, 14–15, 18–21 | 5,927 | 149 | 48 | 6,124 | 5.1 | 17,337 | 5,820 | 33.6 |
| S-3.6 | 3 | 07–10, 13–14, 18–21 | 5,884 | 248 | 46 | 6,178 | 4.2 | 17,148 | 5,721 | 33.4 |

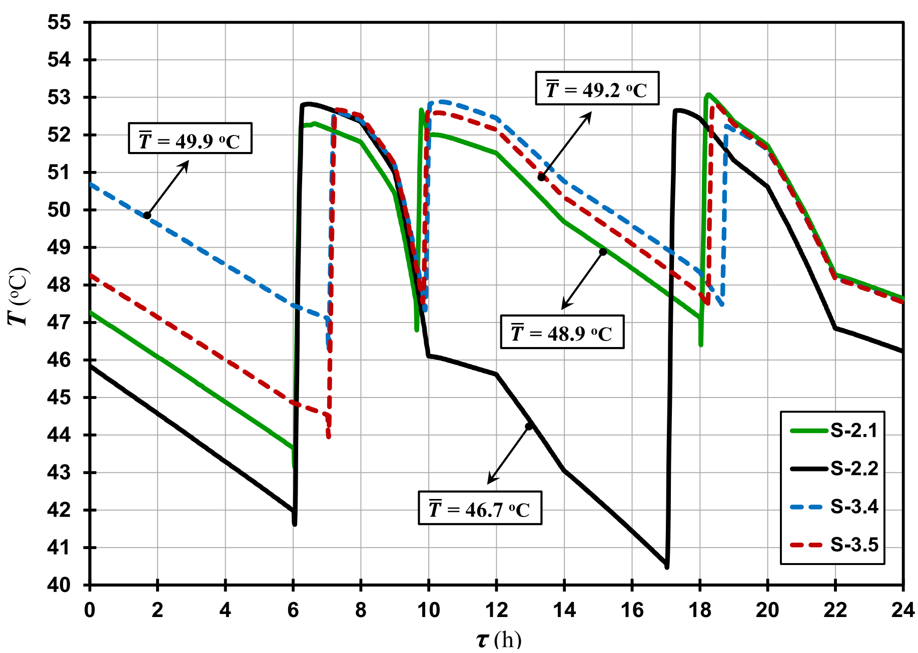


**Fig. 12.** Evaluation of the temperature variation at the DHW outlet port of *e*-TANK (supply) in a typical winter day for four selected charging scenarios.

consumption is amplified in an exponential manner, for both scenarios. For instance, in *S*-3.4, an increment in $T_{ER}$ from 37 to 38 °C leads to 14.1 kWh increase of $E_{el\text{-}ER}$, whereas the same increase in $T_{ER}$ from 40 to 41 °C increases $E_{el\text{-}ER}$ more than 101 kWh, i.e. more than seven times larger consumption. The same trend is also observed for the total electrical energy consumption.

For a given set-point temperature of the *e*-TANK, another parameter in the energy optimisation to be addressed is the adjustment of the main storage's set-point with respect to the heat pump supply temperature. In fact, since the outlet temperature of heat pump varies with the outdoor temperature, the storage's set-point can be given by a constant difference from the supply temperature of heat pump, namely:

$$\Delta T_{s-p} = T_{out,HP} - T_{out,ST} \tag{3}$$

where $T_{out,\ HP}$ and $T_{out,\ ST}$ stand for the fluid temperature at outlet of heat pump and the main storage set-point temperature, respectively.

Fig. 15 illustrates variations in required electrical energy (heat pump and total) and total thermal loss of the DHW system in *S*-3.4 triggered by alterations in $\Delta T_{s\text{-}p}$. The chart indicates that the energy consumption of the system with respect to $\Delta T_{s\text{-}p}$ varies in a quasi-parabolic mode; for the scenario under study, the results show that a ± 1 °C variation in $\Delta T_{s\text{-}p}$ with respect to the optimal case ($\Delta T_{s\text{-}p} = 4.5$ °C) can lead to about 50 kWh electrical energy saving and up to 92 kWh reduction in the thermal loss. To better demonstrate the effect of $\Delta T_{s\text{-}p}$ on minimising the required electrical energy of the heat pump, Fig. 16 compares the hourly profile of the required heat pump energy in a typical winter day for three values of $\Delta T_{s\text{-}p}$. The figure shows that, as selected values of $\Delta T_{s\text{-}p}$ be either closer to the set-point of the heat pump ($\Delta T_{s\text{-}p} = 3.0$ °C) or closer to that of the *e*-TANK ($\Delta T_{s\text{-}p} = 6.0$ °C), the peaks of energy consumption become larger. For instance, at 07:00, the electrical energy required in $\Delta T_{s\text{-}p} = 4.5$ °C is 3.9 and 1.6 kWh smaller than that in $\Delta T_{s\text{-}p} = 6.0$ and 3.0 °C, respectively. Furthermore, the obtained results for other charging scenarios indicate that, for a given $\Delta T_{s\text{-}p}$, the rate of changes in energy consumption may differ to some extent.

### 4.3. The role of user behaviour (draw-off temperature)

In the present section, effects of the user behaviour, regarding the draw-off temperature of DHW, on required annual energy and the fraction of hot/cold water to be mixed are investigated. In this context, three scenarios from each charging scheme were selected, namely *S*-1.1,

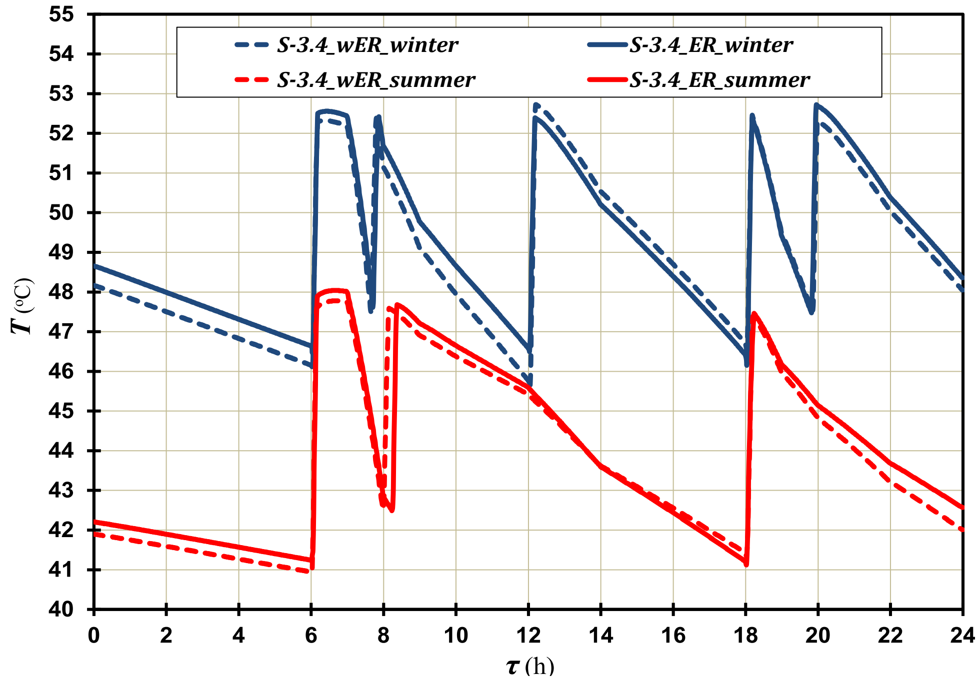


**Fig. 13.** Effect of the proposed auxiliary heater on the daily (winter and summer) DHW temperature profile: *wER* vs. *ER*.

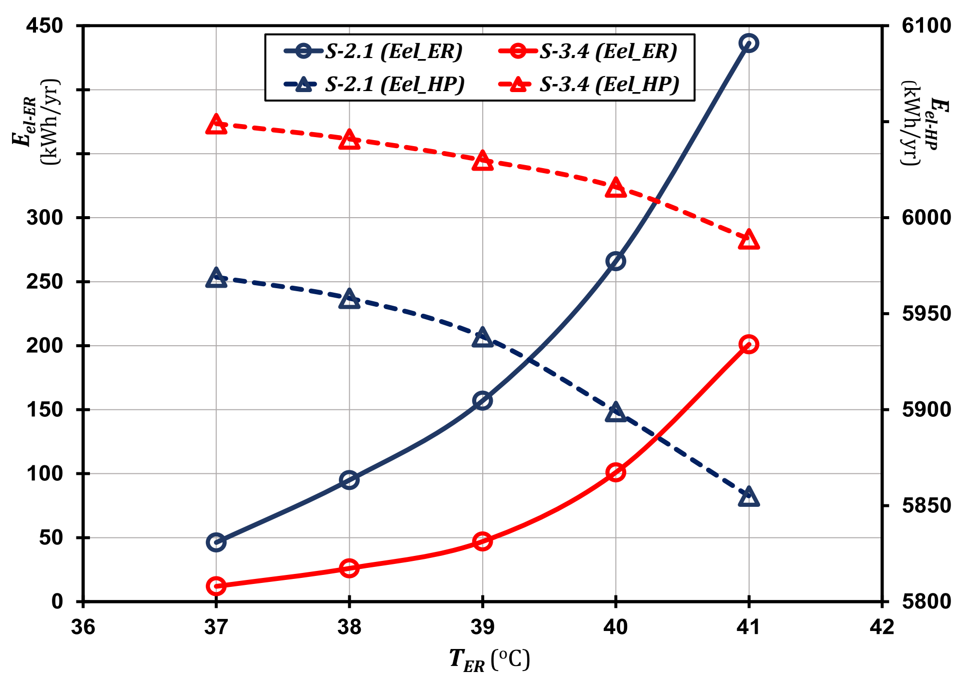


**Fig. 14.** Impact of the set-point temperature of auxiliary electrical heater (by user) on the annual electrical energy consumed by the auxiliary heater and by the heat pump in two different charging scenarios.

*S*-2.2 and *S*-3.4, and a draw-off temperature of DHW were regarded in the range of 37 and 42 °C. To simulate the draw-off temperature by user, a thermostatic valve was inserted into the model in order to mix the hot water discharging from outlet of the *e*-TANK with the aqueduct, at the preferred temperature.

Fig. 17 illustrates the influence of draw-off temperature ($T_{DHW}$) on the required annual energy (kWh/yr) in different charging schemes and on the mean daily proportion of hot/cold water volume per person ($V$). The figure evidently shows the striking impact of a small increase in draw-off temperature of DHW by user on the total required annual energy in any charging scheme. Elaboration of results showed also a similar trend for the energy consumption of the auxiliary heater. Moreover, it can be observed that the rate of changes in the energy consumption by variations in $T_{DHW}$ is not identical for different scenarios. For instance, *S*-2.2 at $T_{DHW}$ = 38 °C requires 19 kWh/yr less energy than *S*-3.4, while energy consumption in *S*-2.2 at $T_{DHW}$ = 42 °C is 53 kWh/yr higher than *S*-3.4. To show this trend quantitatively, the sensitivity of total electrical energy, total heat loss and $CO_2$ emission to the draw-off temperature are reported in Table 2, for various charging schemes and with respect to reference temperature of 37 °C ($\Delta T_{DHW}$).

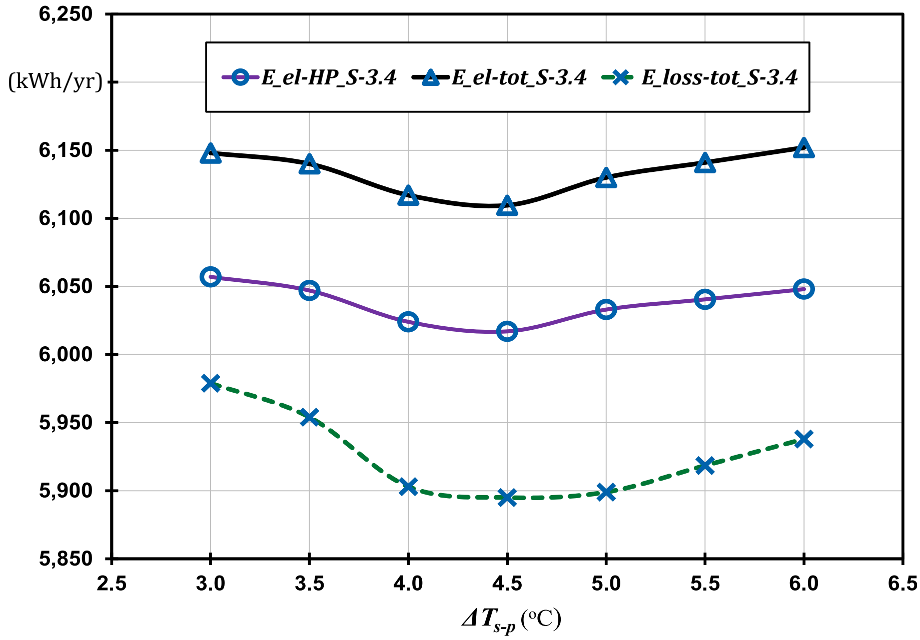


**Fig. 15.** Variations in the required annual electrical energy (heat pump and total) and total thermal loss of the DHW system triggered by alterations in the set-point temperature of central storage.

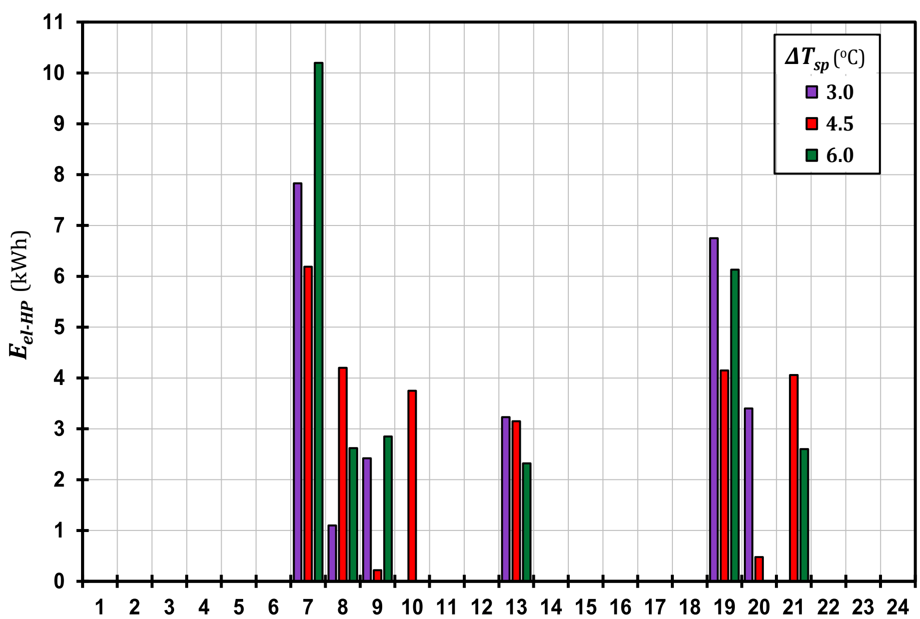


**Fig. 16.** Comparison of the hourly energy consumption profile of heat pump for different set-point temperatures of the central storage.

The table shows that 1 °C increment in $T_{DHW}$ increases on average (in three scenarios) 3.7% total required electrical energy, 0.26% total thermal loss and 94.6 kg the emission of $CO_2$, i.e. 2.96 kg per person. However, it is noticeable that these values can be even higher under charging scenario *S*-2.2.

It should be noted that the elaboration of the results showed that the proportion of $V_H$ and $V_C$ are almost identical in different charging schemes (Fig. 17). Nonetheless, the required hot and cold volume fraction of DHW can be considered as dependent not only upon the draw-off temperature ($T_{DHW}$), but also on the temperature of tank at outlet ($T_H$) and the temperature of aqueduct ($T_C$). According the mean annual aqueduct temperature of pilot building, Fig. 18 demonstrates variations in required hot water fraction ($f_H$), defined as $f_H = V_H / V$, triggered by alterations in values of $T_H$ and $T_{DHW}$. The blue diagrams represent changes in $f_H$ with variations in $T_H$ for given values of $T_{DHW}$, and the red diagrams demonstrate alterations in $f_H$ with variations in $T_{DHW}$ for given supply temperatures of decentralised tank, namely $T_H$.

The figure evidently shows more prominent role of $T_{DHW}$, compared to $T_H$, in variation of the required hot water fraction; for a given $T_H$, the mean rate of changes in hot water fraction by a degree change in $T_{DHW}$ is 5.2%, whereas, for a given $T_{DHW}$, this rate by a degree change in $T_H$ is equal to 3.4%. Moreover, it can be observed that $f_H$ varies linearly with $T_H$ and $T_{DHW}$ in two opposite trends. However, it is noticeable that the net rate of thermal energy required to be supplied to the fluid is

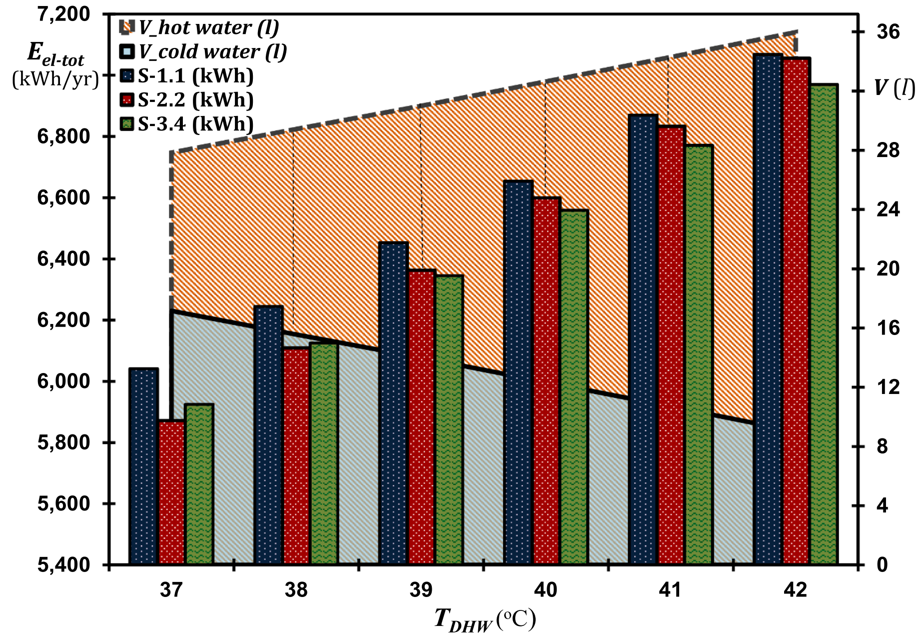


**Fig. 17.** The impact of draw-off temperature (DHW) on required annual electrical energy (kWh/yr) in different charging schemes and on mean daily volume proportion of hot/cold water per person (litres).

**Table 2**
The sensitivity of the total electrical energy, total heat loss and $CO_2$ emission to draw-off temperature under various charging schemes.

| $\Delta T_{DHW}$ | $\delta_{el\text{-}tot}$ (%) | | | $\delta_{loss\text{-}tot}$ (%) | | | $CO_2$ (kg) | | |
|---|---|---|---|---|---|---|---|---|---|
| (°C) | S-1.1 | S-2.2 | S-3.4 | S-1.1 | S-2.2 | S-3.4 | S-1.1 | S-2.2 | S-3.4 |
| 1 | 3.4 | 4.0 | 3.6 | 0.6 | 0.1 | 0.1 | 88.4 | 102.7 | 86.6 |
| 2 | 6.8 | 8.4 | 7.1 | 0.8 | 0.4 | 0.3 | 178.5 | 212.7 | 181.9 |
| 3 | 10.1 | 12.4 | 10.7 | 0.9 | 0.6 | 0.5 | 265.6 | 314.9 | 274.6 |
| 4 | 13.7 | 16.4 | 14.3 | 1.6 | 0.7 | 1.0 | 359.1 | 416.3 | 366.5 |
| 5 | 17.0 | 20.2 | 17.6 | 1.7 | 0.8 | 1.3 | 444.9 | 512.9 | 452.7 |
| Mean | 3.4 | 4.1 | 3.5 | 0.4 | 0.2 | 0.3 | 89.1 | 104.0 | 90.8 |

theoretically independent of the outlet temperature of decentralised tank ($T_H$), and can be considered only as the function of $T_{DHW}$ and $T_C$. To provide an insight into this issue, regarding the first law of thermodynamic in steady-state process, one can write the energy balance equation in the control volume of a thermostatic water tap as:

$$m_H h_H + m_C h_C = m_{DHW} h_{DHW} \quad (4)$$

where $m$ is the mass (kg) and $h$ is the specific enthalpy (J/kg). By substituting the definition of enthalpy and $m_{DHW} = m_H + m_C$ in Eq. (4), it can be rewritten as:

$$m_H(T_H - T_{DHW}) = m_C(T_{DHW} - T_C) \quad (5)$$

Considering $f_H = \rho V_H/m$ and $f_C = \rho V_C/m$, where $\rho$ is the density of water (kg/m$^3$), Eq. (5) becomes:

$$\frac{f_H}{f_C} = \frac{(T_{DHW} - T_C)}{(T_H - T_{DHW})} \quad (6)$$

By replacing $f_C = 1\text{-}f_H$ in Eq. (6), the final form for the required fraction of hot water from tank can be expressed as:

$$f_H = \frac{(T_{DHW} - T_C)}{(T_H - T_C)} \quad (7)$$

Indeed, for a given draw-off temperature ($T_{DHW}$), the required daily thermal energy ($Q$) for heating the water from aqueduct temperature ($T_C$) to tank set-point temperature ($T_H$) can be given by:

$$Q = \rho V f_H c_p (T_H - T_C) \quad (8)$$

where $V$ is the daily DHW consumption per person (m$^3$) and $c_p$ is the specific heat (J/kg.K). If one substitutes Eq. (7) in Eq. (8), it takes the following final form:

$$Q = \rho V c_p (T_{DHW} - T_C) \quad (9)$$

Equation (9) implies that $T_{DHW}$, $T_C$ and $V$ are parameters affecting directly the net thermal energy required from the decentralised storage tank due to fluid exiting through the outlets and entering the tank through the inlets. Nevertheless, it is worthy to mention that variation in decentralised tank set-point temperature (or in $T_H$) may affect the total required thermal energy from the source, i.e. from heat pump to heat exchanger of tank, due to variations in the rate of thermal loss in DHW components.

## 5. Discussion

In the present study, beside the energy analyses of proposed DHW system for the pilot building, it has been attempted to address the influential role of technological aspects in conjunction with the control strategies in energy saving. The role of user behaviour in draw-off temperature was explicitly shown in Section 4.3. However, the role of user behaviour in utilising the auxiliary heater should not be disregarded. Indeed, the concept of utilising auxiliary heater was, firstly, prevention of *legionella pneumophila*, and, then, providing possibilities of having hot water in periods out of the charging slot, according to the adopted charging scheme (see Table 1). In this context, the role of user behaviour can be identified from two aspects: setting the activation

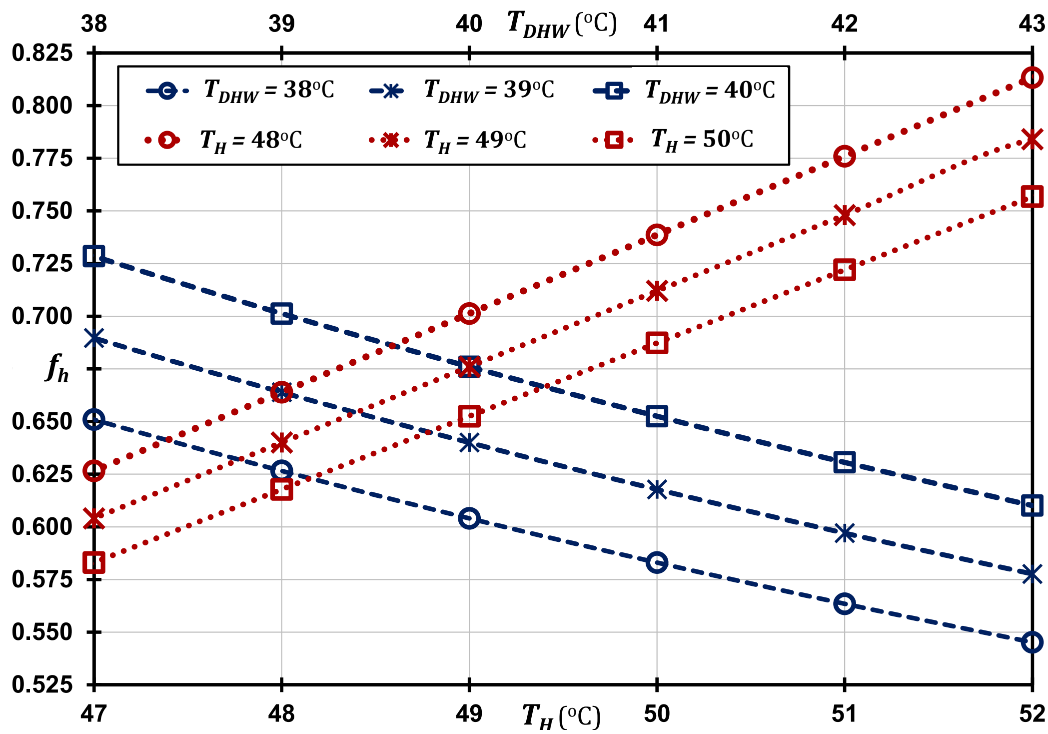


**Fig. 18.** Alterations in hot water fraction ($f_H$) triggered by variations in values of $T_H$ and $T_{DHW}$, for the given aqueduct temperature of pilot building.

temperature of built-in auxiliary heater, as shown in Fig. 14, and also the level of consumption out of the available charging period of circulating pump (mostly at night), i.e. periods in which the *e*-TANK is heated by auxiliary heater.

Regarding the energy performance, comparison of the results yielded by the proposed system with those of previous electrical-decentralised one (see Fig. 10) as well as with the literature data, reported in Table 3, shows that the performance of the proposed system for pilot building can be considered promising. Table 3 compares the mean annual energy required for production of the DHW per person between the pilot case (for four scenarios of Table 1) and the averaged value in European countries (EU), the UK, Canada, and the USA, as reported in [33,38]. For a given mean daily DHW consumption, the daily required energy for DHW production for different countries in [33] has been calculated on the basis of a 45 °C temperature rise for a household, which is slightly higher than the required temperature rise in the pilot case, due to a warmer aqueduct temperature in Catania.

Nevertheless, it should be noted that the required energy for DHW production is significantly dependent upon the mean daily consumption as well as time-dependency of DHW profile. In the present study, the developed MATLAB code for DHW consumption profile takes into account a mean annual value of 45 *l*/person/day with relevant variations in monthly and daily profiles, according to the available literature data. Comparing the measured data for mean DHW consumption of 82 occupants in a European country [39] with that simulated in the present study implies the reliability of MATLAB code for DHW consumption profile; the average value in the measured month (November) for whole group of representative was 47.30 *l*/day/person [39], compared to the simulation results in the present study which is equal to 47.41 *l*/day/person for the same month.

In fact, the mean daily DHW consumption can be globally categorised in a wide range from 20 to 94 *l*/day/person, according to Annex 42 [38]. This wide range may be justified by miscellaneous factors such as the geographical location, number of occupants in a household, gender, age, culture, education, and income, as surveyed in [35]. Therefore, this issue can be considered as the main limitation for studies assessing energy performance of the DHW system in pilot cases, similar to the present study. In this context, the next phase of this study will be devoted to the monitoring of hourly DHW consumption profile in the pilot building and, based on monitored data, the control measures will be updated for a better energy optimisation of the proposed DHW system. Furthermore, considering the economic feasibility of the proposed system, a techno-economic analysis on the proposed retrofit solution will be performed and the outcomes will be compared to those yielded by a typical centralised DHW solution.

## 6. Conclusions

The present study dealt with a multi-objective study on a compound system for domestic hot water (DHW) production in a pilot building, located in Southern Italy. The proposed system consisted of an innovative slim decentralised modular tank (*e*-TANK) to produce and store DHW, connected via a 2-pipe hot water network to a centralised PV-fed air-to-water heat pump system and a thermal energy storage. The dynamic simulations of DHW system were carried out by developing a coupled TRNSYS-MATLAB code, which was calibrated and validated by

**Table 3**
The required annual energy for DHW production per person: Pilot case vs. different countries.

| Required energy for DHW production | Pilot building *S*-0 | *S*-1.1 | *S*-2.1 | *S*-3.4 | Different countries [33,38] EU | UK | Canada | USA |
|---|---|---|---|---|---|---|---|---|
| (kWh/yr/person) | 583.6 | 565.7 | 537.4 | 548.5 | 958.6 | 569.4 | 1788.5 | 762.1 |

experimental data. The energy performance of the proposed system for pilot building was investigated and the optimisation of the results was performed by emphasising on the combined effects of the technological aspects and control strategies. Furthermore, the role of user behaviour in the proposed system for energy saving was addressed.

Comparing the energy performance of the proposed DHW system with the previous decentralized system as well as with the literature data implied the merit of proposed one, both in terms of the energy demand and decoupling energy production. It was shown that the adopted photovoltaic (PV) panels in conjunction with the battery storage increase the renewable energy quota in the proposed system to more than 82%. The optimisation results indicated that employing three times charging scheme (*S*-3.4) is advantageous since it provides a more stable hot water temperature profile as well as a relatively higher temperature. In terms of the energy demand, it was shown that this scheme reduces the required total annual electricity by 5.2 % and enhances total thermal loss from components up to 4.0%, compared to the available-by-demand charging scheme.

The results indicated the striking role of user behaviour in draw-off temperature and pre-defined temperature for activation of the built-in auxiliary heater. It was shown that only a degree increment in draw-off temperature would increase the annual electrical energy consumption by 4.1%, and the annual emission of $CO_2$ by 104 kg, i.e. 3.25 kg per person. The results showed that the increment percentage in energy consumption is amplified in an exponential manner by increasing the set-point of auxiliary heater (up to 101 kwh/yr). Moreover, it was demonstrated that the proposed built-in auxiliary heater is beneficial if it be utilised under an appropriate charging scheme and a plausible pre-defined set-point by users.

## CRediT authorship contribution statement

**Aminhossein Jahanbin:** Conceptualization, Methodology, Software, Validation, Formal analysis, Investigation, Writing – original draft, Writing – review & editing. **Paolo Valdiserri:** Conceptualization, Methodology, Software, Writing – review & editing. **Giovanni Semprini:** Supervision, Visualization, Resources, Funding acquisition, Writing – review & editing.

## Declaration of Competing Interest

The authors declare that they have no known competing financial interests or personal relationships that could have appeared to influence the work reported in this paper.

## Data availability

Data will be made available on request.

## Acknowledgments

The present study was carried out in the framework of the "Energy and seismic affordable renovation solutions" (*e*-SAFE) project, which received funding from the European Union's Horizon 2020 research and innovation programme under grant agreement No. 893135.

## References

[1] N. Anisimova, The capability to reduce primary energy demand in EU housing, Energ. Buildings 43 (10) (2011) 2747–2751.
[2] J. Frijns, J. Hofman, M. Nederlof, The potential of (waste) water as energy carrier, Energ. Conver. Manage. 65 (2013) 357–363.
[3] I. Best, H. Braas, J. Orozaliev, U. Jordan, K. Vajen, Systematic investigation of building energy efficiency standard and hot water preparation systems' influence on the heat load profile of districts, Energy 197 (2020), 117169.
[4] A. Marszal-Pomianowska, C. Zhang, M. Pomianowski, P. Heiselberg, K. Gram-Hanssen, A.R. Hansen, Simple methodology to estimate the mean hourly and the daily profiles of domestic hot water demand from hourly total heating readings, Energ. Buildings 184 (2019) 53–64.
[5] D. Marini, R. Buswell and C. Hopfe, "Estimating waste heat from domestic hot water systems in UK dwellings," in *Int. Build. Perform. Simul. Assoc.*, Hyderabad, India, 2015.
[6] M.Z. Pomianowski, H.H. Johra, A. Marszal-Pomianowska, C. Zhang, Sustainable and energy-efficient domestic hot water systems: a review, Renew. Sustain. Energy Rev. 128 (2020), 109900.
[7] P. Valdiserri, Evaluation and control of thermal losses and solar fraction in a hot water solar system, International Journal of Low-Carbon Technologies 13 (3) (2018) 260–265.
[8] T. Cholewa, A. Siuta-Olcha, R. Anasiewicz, On the possibilities to increase energy efficiency of domestic hot water preparation systems in existing buildings-long term field research, J. Clean. Prod. 217 (2019) 194–203.
[9] J.E. Thorsen, S. Svendsen, K.M. Smith, T. Ommen, M. Skov, Feasibility of a booster for DHW circulation in apartment buildings, Energy Rep. 7 (4) (2021) 311–318.
[10] S. Minetto, Theoretical and experimental analysis of a CO2 heat pump for domestic hot water, Int. J. Refrig 34 (3) (2011) 742–751.
[11] E. Fabrizio, F. Seguro, M. Filippi, Integrated HVAC and DHW production systems for zero energy buildings, Renew. Sustain. Energy Rev. 40 (2014) 515–541.
[12] D. Colaross, P. Principi, Yearly performance of a PV-PCM and water storage for domestic hot water energy demand, Energ. Buildings 274 (2022), 112451.
[13] H. Nagpal, J. Spriet, M. Murali, A. McNabola, Heat recovery from wastewater - a review of available resource, Water 13 (9) (2021) 1274.
[14] F. Huber, G. Neugebauer, T. Ertl, F. Kretschmer, Suitability Pre-Assessment of in-Sewer Heat Recovery Sites Combining Energy and Wastewater Perspectives, Energies 13 (24) (2020) 6680.
[15] V. Tiefenbeck, L. Goette, K. Degen, V. Tasic, E. Fleisch, R. Lalive, T. Staake, Overcoming salience bias: how real-time feedback fosters resource conservation, Manag. Sci. 64 (3) (2018) 983–1476.
[16] A.N. Binks, S.J. Kenway, P.A. Lant, The effect of water demand management in showers on houshold energy use, J. Clean. Prod. 157 (2017) 177–189.
[17] J.Y. Lee, T. Yim, Energy and flow demand analysis of domestic hot water in an apartment complex using smart meter, Energy 229 (2021), 120678.
[18] S.J. Kenway, A. Binks, R. Scheidegger, H.-P. Bader, F. Pamminger, P. Lant, T. Taimre, Household analysis identifies water-related energy efficiency opportunities, Energ. Buildings 131 (2016) 21–34.
[19] Y. Zhang, X. Bai, F.P. Mills, J.C.V. Pezzey, Rethinking the role of occupant behavior in building energy performance: a review, Energ. Buildings 172 (2018) 279–294.
[20] B. Hadengue, E. Morgenroth, T.A. Larsen, Screening innovative technologies for energy-efficient domestic hot water systems, J. Environ. Manage. 320 (2022), 115713.
[21] C. Sebarchievici, I. Sarbu, Performance of an experimental ground-coupled heat pump system for heating, cooling and domestic hot-water operation, Renew. Energy 76 (2015) 148–159.
[22] S. Tadeu, M. Gonçalves, N. Simões, G. Costas, A. Tadeu, Procedure to select combined heating and hot water systems: an expeditious cost optimality approach, Journal of Building Engineering 25 (2019), 100838.
[23] T. Niemela, M. Manner, A. Laitinen, T.M. Sivula, J. Jokisalo, R. Kosonen, Computational and experimental performance analysis of a novel method for heating of domestic hot water with a ground source heat pump system, Energ. Buildings 161 (2018) 22–40.
[24] J.M. Corberan, A. Cazorla-Marín, J. Marchante-Avellaneda, C. Montagud, Dual source heat pump, a high efficiency and cost-effective alternative for heating, cooling and DHW production, International Journal of Low-Carbon Technologies 13 (2018) 161–167.
[25] H. Liu, T. Katsura, K. Nagano, An inverter-driven heat pump with a multi-tubular tube-in-tube heat exchanger for domestic hot water supply, Journal of Building Engineering 54 (2022), 104694.
[26] M. Knapik, Analysis and comparison of methods for the preparation of domestic hot water from district heating system, selected renewable and non-renewable sources in low-energy buildings, E3S Web of Conferences 30 (2018) 03001.
[27] M. Dongellini, S. Falcioni, G.L. Morini, Dynamic simulation of solar thermal collectors for domestic hot water, Energy Procedia 82 (2015) 630–636.
[28] e-SAFE, Energy and Seismic AFfordable rEnovation solutions project. https://esafe-buildings.eu/en/.
[29] EN 14597. Temperature control devices and temperature limiters for heat generating systems. European Committee for Standardization, 2012.
[30] EN 806-1. Specifications for installations inside buildings conveying water for human consumption - Part 1: General. European Committee for Standardization, 2000.
[31] H. Averfalk, E. Möllerström, F. Ottermo, Domestic hot water design and flow measurements, Energy Rep. 7 (2021) 304–310.
[32] DPR. 412/93, "DPR 26 agosto 1993, n. 412. Regolamento recante norme per la progettazione, l'installazione, l'esercizio e la manutenzione degli impianti termici degli edifici, in Attuazione dell'art. 4, comma 4, della L. 9 gennaio 1991, n. 10;," President of the Italian Republic:, Roma, Italy (In Italian), 1993.
[33] E. Fuentes, L. Arce, J. Salom, A review of domestic hot water consumption profiles for application in systems and buildings energy performance analysis, Renew. Sustain. Energy Rev. 81 (2018) 1530–1547.
[34] D. Ivanko, H.T. Walnum, N. Nord, Development and analysis of hourly DHW heat use profiles in nursing homes in Norway, Energ. Buildings 222 (2020), 110070.
[35] M. De Simone, L. Callea, G. Fajilla, Surveys and inferential statistics to analyze contextual and personal factors influencing domestic hot water systems and usage profiles in residential buildings of Southern Italy, Energ. Buildings 255 (2022), 111660.

[36] European Commission, "JRC Photovoltaic Geographical Information System (PVGIS)," https://re.jrc.ec.europa.eu/pvg_tools/en/.
[37] "Indicazioni metodologiche per l'applicazione dei fattori di conversione al metodo di calcolo di cui alla DGR 967/2015 e alla DGR 1275/2015," Regione Emilia-Romagna (in Italian), 2015.
[38] I. Knight, N. Kreutzer, M. Manning, M. Swinton, European and Canadian non-HVAC electric demand and DHW load profiles for use in simulating the performance of residential cogeneration systems, Energy conservation in buildings and community systems, IEA Annex 42 (6) (2007) 84.
[39] A. Ferrantelli, K. Ahmed, P. Pylsy, J. Kurnitski, Analytical modelling and prediction formulas for domestic hot water consumption in residential Finnish apartments, Energ. Buildings 143 (2017) 53–60.